

Driven Magnon-Photon System as a Tunable Quantum Heat Rectifier

C. O. Edet,¹ K. Słowik,² N. Ali,³ and O. Abah⁴

¹*Institute of Engineering Mathematics, Universiti Malaysia Perlis, 02600 Arau, Perlis, Malaysia**

²*Institute of Physics, Faculty of Physics, Astronomy and Informatics,*

Nicolaus Copernicus University in Toruń, Grudziadzka 5/7, 87-100 Toruń, Poland

³*Faculty of Electronic Engineering Technology, Universiti Malaysia Perlis, 02600 Arau, Perlis, Malaysia*

⁴*School of Mathematics, Statistics and Physics, Newcastle University,*

Newcastle upon Tyne NE1 7RU, United Kingdom

(Dated: March 11, 2025)

Controlling the flow of heat in quantum systems or circuits is very desirable for the development of quantum technologies. Here, we investigate the quantum heat transport in a driven hybrid magnon-photon system in contact with two thermal baths operating at different temperatures. Specifically, we analyze the role of the parameters of the hybrid quantum system in the processes that lead to the asymmetry of the steady-state heat current. We find that the thermal rectification is high in the regime of weak magnon-photon hybridization strength and large magnon-drive. Moreover, this driving and the system parameters could serve as experimental knobs to tune the thermodynamic properties of the magnon-photon system, as we demonstrate for the rectification parameter tunable by the drive in its entire physical range. The results from this research would provide very useful insight into the design of quantum thermal machines with a driven magnon-photon system.

I. INTRODUCTION

In the quest to miniaturize electronic devices, regulation of heat transport at the nanoscale remains tremendous impediment for the advancement of quantum and classical computing architecture [1]. The rapid progress in quantum technology has led to the need for alternative information carriers, such as magnetic (spin) [2–4] and thermal (phonon) [5–7] currents that are being explored alongside traditional charge carriers. The thermal current, central to thermodynamics, behaves differently at the quantum scale, governed by quantum mechanics. Moreover, minimizing heat dissipation and exploiting the control of heat currents in quantum systems are important for applications in the area of quantum information processing [8], designing quantum thermal devices [9–12], heat transistors [13–20], and thermal rectifiers [1, 21–32].

Theoretical [33–39] and experimental [1, 40] studies on quantum thermal rectifiers are area of current research. The thermal rectifier is a device in which the direction of the heat current is reversed when there is a thermal bias due to the asymmetry and nonlinearity in the physical systems [30, 41]. We remark, for two bosonic thermal reservoirs, a simple two-level system can act as a heat rectifier, while that is not the case for linearly coupled harmonic oscillator [42, 43]. The quantum segmented XXZ chains show strong heat current rectification, emanating from the asymmetry created by different on-site magnetic fields, driving field amplitude, and the coupling strength of the system with their individual baths [44–46]. A giant rectification has recently been proposed in a

one-dimensional lattice of spinless fermions in a tilted potential based on the asymmetric interplay between strong particle interactions and a tilted potential [47]. Heat rectifiers have been investigated in different platforms; solid state quantum circuits [48], coupled two-level atoms [32, 35], quantum dots [49, 50], or superconducting circuit quantum electrodynamics [51].

Furthermore, hybrid magnonic systems have shown great potential for the development of novel quantum technologies [52–56]. Magnons, the collective spin excitation in yttrium iron garnet (YIG), have been coupled with microwave photons through the magnetic dipole [57], optical photons via the magneto-optical effect [58], superconducting quantum circuits indirectly through the mediation of microwave cavity photons [59], among others. A plethora of interaction mechanisms allows the engineering of coherent interactions between distinct systems [60]. In addition, hybrid quantum-magnonic systems provide opportunities for the development of quantum technologies useful in quantum sensing [61], quantum information processing [54], and understanding the interplay between irreversibility and quantum information in a mesoscopic quantum system [62]. Motivated by the versatile nature of the hybrid driven magnonic system, we extend its quantum thermal applications.

In the present study, we introduce a class of tunable quantum rectifiers that utilizes the quintessential parameter of a driven magnon-photon system. Specifically, we investigate the heat current and rectification in a magnon-photon system where the magnon mode is driven; see Fig. 1. The forward heat current \mathcal{J}_m^f is induced by a positive temperature bias ($T_m > T_c$), while the reverse heat current \mathcal{J}_m^r arises from a negative temperature bias ($T_c > T_m$). When the left-right (magnon-photon) symmetry is broken, the magnitude of the heat

* collinsokonedet@gmail.com

current \mathcal{J}_m^f may be different with respect to the magnitude of \mathcal{J}_m^r . We demonstrate that the asymmetry can be induced in a driven magnon-photon system, and by extension, we demonstrate that heat rectification in such a system is possible. We find that the presence of the magnon drive results in finite heat current even for small coupling strength. The control knob, magnon drive field offers the capability of observing full range of rectification in the setup. Moreover, our analytical results for both heat currents and rectification reveals the underlying mechanism that leads to thermal rectification. The

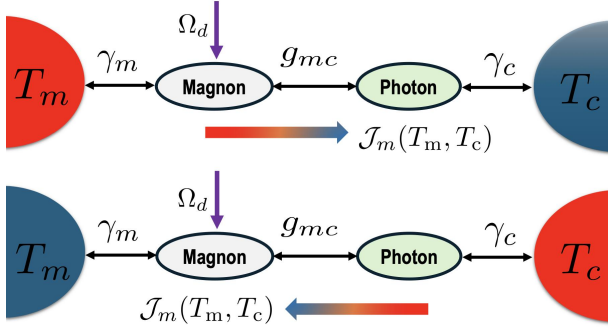


Figure 1. Heat rectification architecture of a driven hybrid magnon-photon system coupled to two different heat reservoirs at fixed temperatures (T_m and T_c) with system-bath couplings γ_m and γ_c . The magnon mode is driven with a driving field of strength Ω_d and the magnon-photon coupling strength g_{mc} . (Top) forward-bias configuration; (bottom) reversed-bias configuration.

structure of the paper is as follows. We introduce the model of the hybrid system and their dissipation as well as derive the open system dynamics evolution equations in Sec. II. In Sec. III, we show the dependence of the heat current on the parameters of the magnon-photon system, and demonstrate that heat rectification can be achieved in such a system by driving the magnon mode. In Sec. IV, we present the experimental feasibility of the proposed quantum thermal rectifier in current state-of-the-art cavity magnonic systems. Finally, the conclusion is given in Sec. V.

II. MODEL AND DISSIPATIVE DYNAMICS

We consider a hybrid quantum system consisting of coherently coupled magnons and microwave photons, which are connected to two different thermal reservoirs, as shown in Fig. (1). The magnons are directly driven by a field, and couple to the cavity photons via the magnetic dipole interaction [54]. The total Hamiltonian of the driven hybrid magnon-photon system is given by

[57, 63, 64];

$$\hat{H}/\hbar = \omega_c \hat{c}^\dagger \hat{c} + \omega_m \hat{m}^\dagger \hat{m} + g_{mc} (\hat{c} \hat{m}^\dagger + \hat{c}^\dagger \hat{m}) + i\Omega_d (\hat{m}^\dagger e^{-i\omega_d t} - \hat{m} e^{i\omega_d t}), \quad (1)$$

where $\hat{c}(\hat{c}^\dagger)$ and $\hat{m}(\hat{m}^\dagger)$ are the annihilation (creation) operators for the photon and magnon modes respectively. The first two terms are the bare Hamiltonians of the microwave cavity and the magnon with frequencies ω_c and ω_m , respectively. The third term denotes the interaction between the photon and the magnon with the coupling strength g_{mc} , which can be adjusted by varying the direction of the bias field or the position of the YIG sphere inside the cavity [54, 57]. The last term represents the magnon mode drive with the amplitude strength Ω_d and the driving frequency ω_d . Making a unitary transformation of the form $\hat{U} = \exp(i\omega_d (\hat{m}^\dagger \hat{m} + \hat{c}^\dagger \hat{c})t)$, in a rotating frame at the magnon driving ω_d , the effective Hamiltonian of Eq. (1) reads $\hat{H}_{\text{eff}} = \hat{U} \hat{H} \hat{U}^\dagger - i\hbar \hat{U} (\partial \hat{U}^\dagger / \partial t)$,

$$\hat{H}_{\text{eff}}/\hbar = \Delta_c \hat{c}^\dagger \hat{c} + \Delta_m \hat{m}^\dagger \hat{m} + g_{mc} (\hat{c} \hat{m}^\dagger + \hat{c}^\dagger \hat{m}) + i\Omega_d (\hat{m}^\dagger - \hat{m}) \quad (2)$$

where $\Delta_c = \omega_c - \omega_d$ and $\Delta_m = \omega_m - \omega_d$ represent the detuning of the photonic and magnonic modes from the drive, respectively.

We assume that the heat reservoirs are Markovian, and the dynamics of the joint system and the reservoirs can be described by the Lindblad-Gorini-Kossakowski-Sudarshan master equation [65, 66]. Thus, the adjoint master equation for the hybrid magnon-photon setup is written as [67]

$$d\hat{O}_H/dt = i[\hat{H}_{\text{eff}}, \hat{O}_H(t)] + \mathcal{L}[\hat{O}](\hat{O}_H) \quad (3)$$

where $\hat{O}_H(t)$ is the Heisenberg-picture operator at time t , and the second term,

$$\begin{aligned} \mathcal{L}[\hat{O}](\hat{O}_H) = & \sum_k \gamma_k (n_k + 1) \left(\hat{O}^\dagger \hat{O}_H \hat{O} - \frac{1}{2} \hat{O}_H \hat{O}^\dagger \hat{O} - \frac{1}{2} \hat{O}^\dagger \hat{O} \hat{O}_H \right) \\ & + \sum_k \gamma_k n_k \left(\hat{O} \hat{O}_H \hat{O}^\dagger - \frac{1}{2} \hat{O}_H \hat{O} \hat{O}^\dagger - \frac{1}{2} \hat{O} \hat{O}^\dagger \hat{O}_H \right) \end{aligned} \quad (4)$$

is the adjoint dissipator [68], which is a superoperator acting on observables \hat{O}_H . Here, γ_k are the strength of the interaction with the reservoirs, $n_k(\omega_k, T_k) = (\exp(\hbar\omega_k/k_B T_k) - 1)^{-1}$, $k \in \{m, c\}$ are the mean number of excitations in the reservoir damping the mode, T_k is the temperature of the coupled bath, and k_B is the Boltzmann constant. The dissipator term represents the interaction of the system with the two environmental heat baths and accounts for the loss of photons/magnons to the coupled heat reservoirs. From Eq. (3), the modes mean-values reads,

$$\frac{d\langle \hat{c} \rangle}{dt} = -i\Delta_c \langle \hat{c} \rangle - ig_{mc} \langle \hat{m} \rangle - \frac{\gamma_c}{2} \langle \hat{c} \rangle, \quad (5)$$

$$\frac{d\langle \hat{m} \rangle}{dt} = -i\Delta_m \langle \hat{m} \rangle - ig_{mc} \langle \hat{c} \rangle - \frac{\gamma_m}{2} \langle \hat{m} \rangle + \Omega_d. \quad (6)$$

Moreover, studying the hybrid quantum setup thermodynamic properties requires the second moments of the mode operators. These reads

$$\frac{d\langle\hat{c}^\dagger\hat{c}\rangle}{dt} = ig_{mc}(\langle\hat{m}^\dagger\hat{c}\rangle - \langle\hat{c}^\dagger\hat{m}\rangle) + \gamma_c(n_c - \langle\hat{c}^\dagger\hat{c}\rangle), \quad (7)$$

$$\begin{aligned} \frac{d\langle\hat{m}^\dagger\hat{m}\rangle}{dt} &= ig_{mc}(\langle\hat{c}^\dagger\hat{m}\rangle - \langle\hat{m}^\dagger\hat{c}\rangle) + \Omega_d(\langle\hat{m}^\dagger\rangle + \langle\hat{m}\rangle) \\ &+ \gamma_m(n_m - \langle\hat{m}^\dagger\hat{m}\rangle), \end{aligned} \quad (8)$$

This demonstrates that the population of each mode is explicitly impacted by $\langle\hat{m}^\dagger\hat{c}\rangle$, representing the excitation hopping between the magnon and photon modes. The hopping excitation is given by

$$\begin{aligned} \frac{d\langle\hat{c}^\dagger\hat{m}\rangle}{dt} &= i(\Delta_c - \Delta_m)\langle\hat{c}^\dagger\hat{m}\rangle + ig_{mc}(\langle\hat{m}^\dagger\hat{m}\rangle - \langle\hat{c}^\dagger\hat{c}\rangle) \\ &+ \Omega\langle\hat{c}^\dagger\rangle - \left(\frac{\gamma_c}{2} + \frac{\gamma_m}{2}\right)\langle\hat{c}^\dagger\hat{m}\rangle. \end{aligned} \quad (9)$$

Solving the complete set of Eqs. (5) - (9) for the steady states by setting $d\langle\dots\rangle/dt = 0$, symmetric bath-system coupling ($\gamma_m = \gamma_c = \gamma$) and detunings ($\Delta_m = \Delta_c = \Delta$), we obtain the expectation values as;

$$\langle\hat{c}^\dagger\hat{c}\rangle = \frac{2g_{mc}^2(n_m - n_c)}{\gamma^2 + 4g_{mc}^2} + \frac{g_{mc}^2\Omega_d^2}{\Xi} + n_c \quad (10)$$

$$\langle\hat{m}^\dagger\hat{m}\rangle = \frac{\Omega_d^2\left(\Delta^2 + \frac{\gamma^2}{4}\right)}{\Xi} + \frac{2g_{mc}^2(n_c - n_m)}{\gamma^2 + 4g_{mc}^2} + n_m, \quad (11)$$

$$\langle\hat{c}^\dagger\hat{m}\rangle = i\left(g_{mc}\Omega_d^2\frac{\left(\frac{\gamma}{2} + i\Delta\right)}{\mathcal{R}} + \frac{g_{mc}\gamma}{\gamma^2 + 4g_{mc}^2}(n_m - n_c)\right), \quad (12)$$

where $\Xi = \left(g_{mc}^2 - \Delta^2 + \frac{\gamma^2}{4}\right)^2 + \Delta^2\gamma^2$.

III. THERMODYNAMIC ANALYSIS

In this section, we analyze the heat transport and rectification coefficient of the driven-dissipative magnon-photon system. Specifically, we will focus on how these quantities are affected by the system parameters.

A. Heat Current

Now, we focus on the steady-state heat current that flows across the device when a temperature bias is imposed between the heat reservoirs. At steady state, the heat current flowing into the magnon or photon mode from its coupled heat reservoir can be defined as [26, 27, 69]

$$\mathcal{J}_i = \gamma_i\Delta_i(n_i - \langle\hat{i}^\dagger\hat{i}\rangle), \quad (13)$$

where \mathcal{J}_i , $i = m, c$ is the rate of heat current flowing from each reservoir to the system, and $\langle\hat{i}^\dagger\hat{i}\rangle$ is the second moments of the operator/mode (see, Eqs. (10) - (11)). Considering symmetric system and reservoir couplings $\gamma_m = \gamma_c = \gamma$ as well as frequency detunings, $\Delta_m = \Delta_c = \Delta$, the heat currents are respectively calculated in a compact form as;

$$\mathcal{J}_m = -\gamma\Delta\left(\frac{\Omega_d^2\left(\Delta^2 + \frac{\gamma^2}{4}\right)}{\Xi} - \frac{2g_{mc}^2}{\gamma^2 + 4g_{mc}^2}(n_m - n_c)\right) \quad (14)$$

and

$$\mathcal{J}_c = -\gamma\Delta\left(\frac{\Omega_d^2g_{mc}^2}{\Xi} + \frac{2g_{mc}^2}{\gamma^2 + 4g_{mc}^2}(n_m - n_c)\right). \quad (15)$$

Equations (14) and (15) are the exact steady state heat currents of dissipative driven hybrid photon-magnon when the system-reservoir couplings and the frequency detunings are symmetric. It clearly shows that there is still energy current flow for vanishing coupling between the modes due to the driving of the magnon mode. Hence, the non-conservation of heat currents, that is, $\mathcal{J}_m \neq -\mathcal{J}_c$, results from the asymmetry created by the finite magnon drive $\Omega_d \neq 0$. When $\Omega_d = 0$, the current is still finite, and we recover the result in [68]. Furthermore, as expected from fundamental thermodynamics that heat will always flow from hot to cold bath, the heat current \mathcal{J}_m increases with temperature gradient (i.e., $n_m - n_c$) and its magnitude depends on whether the magnon bath is hotter than the photon bath or vice versa. As depicted in Fig. (1), forward bias (reverse bias), the heat current \mathcal{J}_m^f (\mathcal{J}_m^r) flows from the magnon to the photon bath (photon to magnon) when $T_m > T_c$ ($T_c > T_m$) with T_m (T_c) denotes the temperature of the magnon (photon) bath. The positive value of the heat current represents the flow of heat from the bath to the system and vice versa.

We further analyze the heat current with more emphasis on its tunability with the driving amplitude Ω_d , detuning Δ , and the temperatures of the heat reservoir. Without loss of generality, we focus on the forward-bias magnon heat current in our analysis. That is, $\mathcal{J}_m \equiv \mathcal{J}_m^f$, unless otherwise stated. In Fig. 2(a), we show the plot of the forward bias magnon heat current against the temperature of the magnon heat bath in the absence of the magnon driving, $\Omega_d = 0$, for different values of detuning, Δ . The heat current increases linearly with increasing temperature and detuning Δ . However, when the magnon mode is driven, $\Omega \neq 0$, the heat current is reversed in the region $T_m \equiv T < 1$, as shown in Fig. 2(b). This is an example how the presence of sufficiently strong drive can flip the sign of the current, as it follows directly from Eqs. (14) and (15). Moreover, increasing the detuning linearly improves the magnitude of the heat current, except for the temperature range $T_m \leq 1$, where the behavior is more complicated. Fig. 2 (c) shows that the forward bias heat current is inversely related to the corresponding reverse bias case. We further observe that

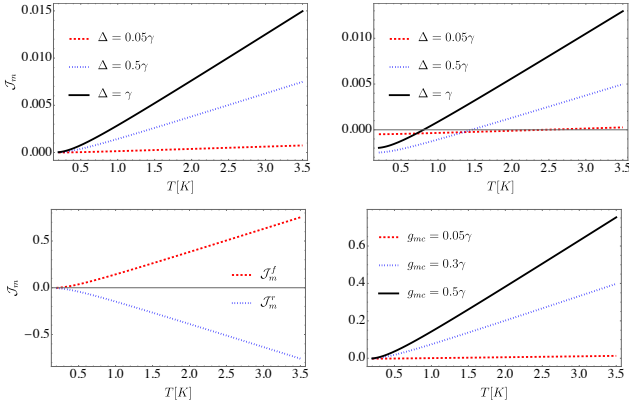


Figure 2. Steady-state magnon heat current \mathcal{J}_m as a function of reservoir temperature $T[K]$ for different detuning Δ , driving field strength Ω_d , and coupling strength g_{mc} . (a) Magnon heat current \mathcal{J}_m as a function of $T_m = T$ for different detuning; $\Delta = 0.05\gamma$ (red dashed line), $\Delta = 0.5\gamma$ (blue dotted line), and $\Delta = \gamma$ (black solid line) with $\Omega_d = 0$, $T_c = 0.1$ and $g_{mc} = 0.05\gamma$. (b) Same as (a), but with the driving strength $\Omega_d = 0.05\gamma$. (c) \mathcal{J}_m as a function of temperature T with $g_{mc} = 0.5\gamma$, $\Omega_d = 0.05\gamma$ and $\Delta = \gamma$. For forward bias case, we assumed $T_c = 0.1$ and $T_m = T$ while the reverse bias case, $T_c = T$ and $T_m = 0.1$. (d) \mathcal{J}_m versus temperature $T \equiv T_m$ for different magnon-photon coupling; $g_{mc} = 0.05\gamma$ (red dashed line), $g_{mc} = 0.3\gamma$ (blue dotted line), and $g_{mc} = 0.5\gamma$ (black solid line) with $\Omega_d = 0.05\gamma$ and $\Delta = \gamma$. Other parameters are chosen as $\Delta_m = \Delta_c = \Delta$ and $\gamma_c = \gamma_m = \gamma = 1$.

by increasing the magnon-photon hybridization strength from weak to strong for non-zero magnon driving, the heat current increases, as shown in Fig. 2(d). In summary, Fig. 2 shows that; (i) The magnitude of the heat current \mathcal{J}_m depends on the parameters of the hybrid system (Δ and g_{mc}), but more strongly on the driving strength of the microwave field which may alter its direction or magnitude. In the absence of magnon mode driving, the direction of heat current only changes with the interchange of heat bath temperatures (this can be confirmed from the analytical expressions in Eqs. (14) and (15)). (ii) For forward bias, in the absence of driving $\Omega_d = 0$, the steady-state heat current \mathcal{J}_m^f is positive, that is, the heat current flows from the magnon mode to the photon mode irrespective of the parameters of the system (although the presence of the drive alters the magnitude and captures regimes below zero). In the reverse bias case, the heat current \mathcal{J}_m^r is negative and in the opposite direction. (iii) For very weak magnon-photon coupling $g \simeq 0.005\gamma$, the negative magnitude of the heat current \mathcal{J}_m begins to dominate. (iv) In the presence of the magnon mode driving, the heat current is still sustained even when the mode hybridization strength tends to vanish, $g_{mc} \simeq 0$. Fig. 3(a) show that high-temperature bias and strong magnon-photon hybridization are associated with enhanced heat current. In Fig. 3(b), we see that the relatively strong drive can suppress the heat current. The detunings for which this suppression is most effective

are functions of the system parameters, in particular the magnon-photon coupling strength, as seen in Fig. 3(c). The capability of magnon mode drive to reverse the direction of flow of the heat current is further demonstrated in Fig. 3(c) in a range of coupling strengths. Once again, this demonstrates that the drive can be used as a knob to tune the amplitude and direction of the heat current.

B. Heat Rectification

Now, we present how to utilize the turnability of the driven hybrid magnon-photon quantum system to construct a heat rectifier. The hybrid quantum system operates as a heat rectifier when there is asymmetric flow of heat current due to the dependence of its magnitude on the temperature gradient [33]. Thus, the heat rectification coefficient can be described as the asymmetry of the heat current subject to the forward and reverse directions, and it can be quantitatively described as; [70, 71],

$$\mathcal{R} = \frac{|\mathcal{J}_m^f + \mathcal{J}_m^r|}{\max(|\mathcal{J}_m^f|, |\mathcal{J}_m^r|)}, \quad (16)$$

where \mathcal{J}_m^f (\mathcal{J}_m^r) correspond to the heat current in the forward (reverse) bias configuration, see Fig. 1. From Eq. (16), $0 \leq \mathcal{R}(\mathcal{J}_m^f, \mathcal{J}_m^r) \leq 2$, the lower bound is when there is symmetrical flow of the heat current, $\mathcal{J}_m^f = -\mathcal{J}_m^r$; while the upper bound saturates for heat fluxes that are independent of the temperature gradient, $\mathcal{J}_m^f = \mathcal{J}_m^r$. In Fig. 4, we show the dependence of the rectification coefficient \mathcal{R} on the magnon-photon coupling strength g_{mc} , detuning Δ , and magnon heat bath temperature $T_m = T$. In Fig. 4(a), we see that heat rectification reduces with increasing coupling strength g_{mc} , in agreement with the results of the two-coupled qubit setup [27]. On the other hand, the heat rectification is high and non-zero throughout the regime of detuning Δ considered. Figures 4 (b) and (c) show that when other parameters of the hybrid system and the temperature of the heat baths are fixed, adjustment of the drive amplitude Ω_d allows one to control the rectification parameter in the full range between 0 and 2. We observe the capability of the setup to attain $\mathcal{R} = 1$, which indicates that the heat flux \mathcal{J}_m is completely suppressed in one of the configurations. The regions with non-zero rectification correspond to regions with non-zero driving Ω_d and the maximum values of the heat rectification achieved in the regime $\Omega_d > 0.5\gamma$. In the low-temperature bias regime, the rectification factor \mathcal{R} is seen to be finite from weak to strong magnon driving amplitude, as shown in Fig. 4(c).

To gain more insight, an analytical expression for the rectification is obtained using Eq. (16), it reads;

$$\mathcal{R} = \frac{4\Omega_d^2 (\gamma^2 + 4\Delta^2) (\gamma^2 + 4g_{mc}^2)}{2\Omega_d^2 (\gamma^2 + 4\Delta^2) (\gamma^2 + 4g_{mc}^2) + g_{mc}^2 (n_c - n_m) \tilde{\mathcal{G}}_0} \quad (17)$$

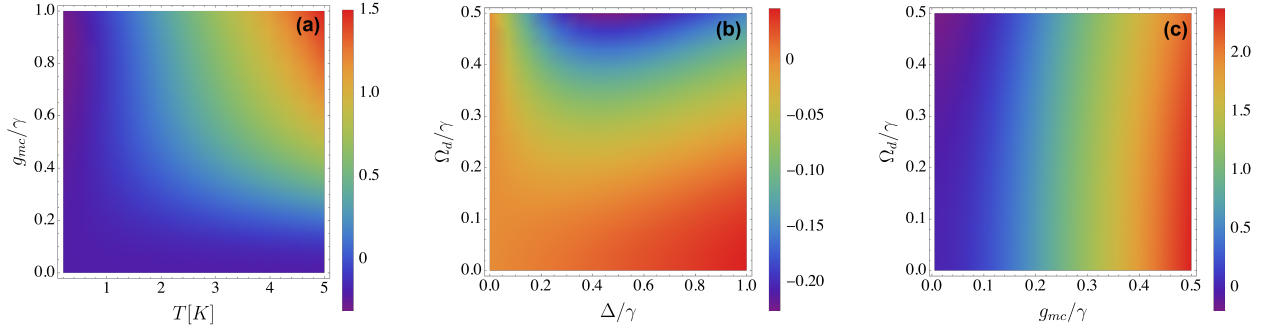


Figure 3. Steady-state magnon heat current (forward bias) dependence on the hybrid system parameters and magnon heat reservoir temperature. (a) \mathcal{J}_m as a function of the coupling strength g_{mc}/γ and magnon heat bath temperature $T_m = T$ with $\Delta = \gamma$ and $\Omega_d = 0.5\gamma$. (b) \mathcal{J}_m as a function of driving amplitude Ω_d/γ and detuning Δ/γ with $g_{mc} = 0.05\gamma$ and $T_m = 10$. (c) \mathcal{J}_m as a function of Ω_d/γ and magnon-photon coupling strength g_{mc}/γ with $\Delta = \gamma$ and $T_m = 10$. Other parameters are the same as in Fig. 2.

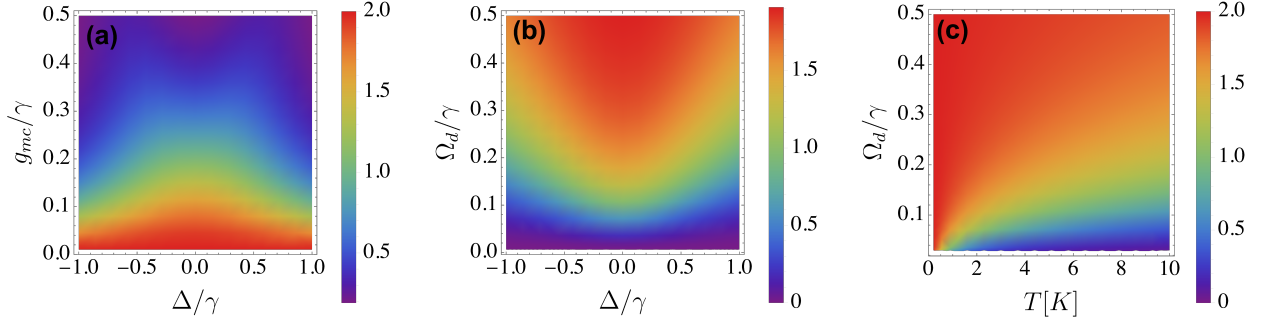


Figure 4. (a) Rectification coefficient \mathcal{R} as a function of magnon-photon coupling g_{mc} and detuning Δ with driving amplitude $\Omega_d = 0.5\gamma$. (b) Rectification coefficient \mathcal{R} as a function of the strength of the magnon driving Ω_d and detuning Δ with $g_{mc} = 0.05\gamma$. (c) \mathcal{R} as a function of the strength of the magnon driving Ω_d and magnon heat bath temperature $T_m = T$ with $g_{mc} = 0.05\gamma$, $\Delta = 0.5\gamma$, and $T_c = 0.1$. In (a) and (b), the temperatures are $T_c = 0.1$ (low) and $T_m = 10$ (high). Other parameters are the same as in Figs. (2).

where $\tilde{\mathcal{G}}_0 = (\gamma^2 + 4(g_{mc} - \Delta)^2)(\gamma^2 + 4(\Delta + g_{mc})^2)$. Equation (17) shows that rectification can only be realized at non-zero drive amplitude and, in the weak-drive regime, it scales linearly with its intensity. Expanding Eq. (17) in a power series of Δ , we get

$$\mathcal{R} \approx \frac{4\gamma^2\Omega_d^2}{2\gamma^2\Omega_d^2 + 4g_{mc}^4(n_c - n_m) + \gamma^2g_{mc}^2(n_c - n_m)} + O(\Delta^2). \quad (18)$$

From Eq. (18), We see that even for a sufficiently small coupling strength g_{mc} , the rectification is still sustained. Moreover, in the regime of weak g_{mc} , we can recover the upper of bound $\mathcal{R} \approx 2$. Furthermore, studies have shown that there is a trade-off between heat current and heat rectification [30, 45]. To this end, we present a comparison between the rectification and maximum heat current as a function of the magnon temperature of the heat reservoir $T_m \equiv T$ in Fig. (5). From this plot, it is explicitly demonstrated that the highest \mathcal{R} occurs in the region where $\mathcal{J}_{\max} = \max\{\mathcal{J}_m^f, \mathcal{J}_m^r\}$ is the lowest. We observe

that the rectification factor (heat current) of the hybrid quantum setup is enhanced (reduced) in the low temperatures region. This implies that a high heat current corresponds to lower rectification factors and vice versa, in agreement with the previous study on the quantum thermal device [19, 30].

IV. EXPERIMENTAL REALIZATION

Here, we discuss the possible implementation of a magnon-photon system as a quantum heat rectifier. Such a setup would include a three-dimensional (3D) microwave cavity and a well-polished Yttrium iron garnet (YIG) sphere; the YIG functions as the magnon cavity. The cavity is a box fabricated from highly conductive copper to achieve a high-quality factor at room temperature [57]. Then, the YIG sphere is placed inside the microwave cavity and biased with a static magnetic field.

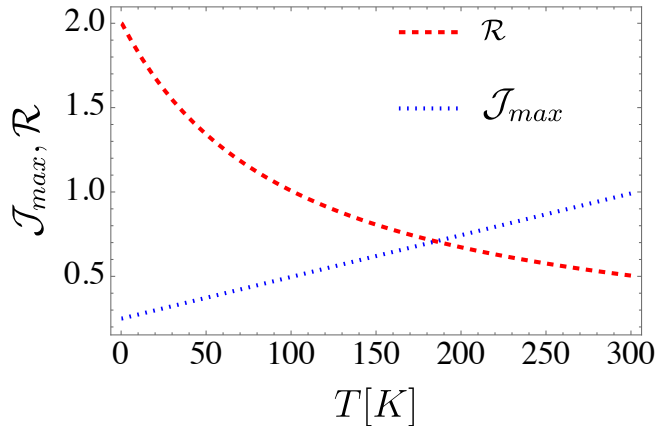


Figure 5. Comparison between the Rectification \mathcal{R} (red curve) and $\max\{\mathcal{J}_m^i, \mathcal{J}_m^r\}/\gamma\Delta$ against magnon bath temperature $T_m \equiv T$. The parameters used are: $g_{mc} = 0.05\gamma$, $\Omega_d = 0.5\gamma$, $\Delta = 0.5\gamma$, $T_c = 0.1$ and $\gamma = 1$.

The magnetic components of the microwave field are perpendicular to the bias field which induces the spin-flip and thus excites the magnon mode in YIG. The lowest order ferromagnetic resonance mode consists of a uniform collective mode, in which all the spins precess in phase. This mode has the highest coupling strength given that the microwave magnetic field around the YIG sphere is approximately uniform as the wavelength $\lambda_{mw} \gg R$, where R is the radius of the YIG sphere. The frequency of the uniform magnon mode linearly depends on the bias field: $\omega_m = \gamma_{gr}|B_0| + \omega_{m,0}$, where γ_{gr} is the gyromagnetic ratio and $\omega_{m,0}$ is determined by the anisotropy field. The bias magnetic field is tunable in the range of 0–2 Tesla, corresponding to a magnon frequency from a few hundred MHz to about 50 GHz. This ability to tune the resonance frequency of the magnon mode could serve as an additional resource to achieve heat rectification (asymmetry) in the setup. To achieve the photon-magnon interaction, the bias field is adjusted such that the magnon is near resonance with the photon mode. The strongest interaction coupling strength is obtained by placing the YIG sphere at the position with the maximum microwave magnetic field [57, 63, 64], which have been implemented in recent experiments [53, 57]. This demonstrates the fact that the setup is a useful resource for the imple-

mentation of a controllable quantum heat rectifier. Finally, some experimentally feasible parameters to implement the scheme as follows: the strong coupling between the microwave photon and the magnon, with the coupling strength $g_{mc}/2\pi = 10.8\text{MHz}$, the dissipation rates of the microwave photon and the magnon are respectively $\gamma_c/2\pi = 2.67\text{MHz}$ and $\gamma_m/2\pi = 2.13\text{MHz}$, and the resonance frequency of the photon $\omega_c/2\pi = 10\text{GHz}$ [57, 72].

V. CONCLUSION

We have investigated heat transport and heat rectification in a driven dissipative magnon-photon system. The system is in contact with two fixed temperature reservoirs. Employing the Lindblad master equation formalism for an open quantum system, we derived analytical expressions for the steady-state heat current and identified the key mechanisms responsible for asymmetry in heat transport. The external magnon drive was found to play a pivotal role, not only in inducing asymmetry but also in serving as a powerful tuning parameter for the hybrid quantum system thermal response.

These results highlight the significant potential of driven hybrid magnon-photon systems in the advancement of the design of quantum thermal devices, including thermal rectifiers, thermal diodes, and thermal transistors. Furthermore, our work opens new avenues for exploring quantum control strategies in heat transport, offering a promising platform for future research into quantum thermal machines and energy-efficient quantum technologies.

ACKNOWLEDGEMENTS

COE and NA acknowledge support from the Long Term Research Grant Scheme (LRGS) with grant number LRGS/1/2020/UM/01/5/2 (9012-00009), provided by the Ministry of Higher Education of Malaysia (MOHE). KS acknowledges the National Science Centre, Poland, project number 2020/39/I/ST3/00526. Part of this project was carried out during COE’s visit to Nicolaus Copernicus University (NCU) in Torun, and he acknowledges the support of the NCU’s Research University Centre of Excellence “From Fundamental Optics to Applied Biophotonics”.

-
- [1] J. Senior, A. Gubaydullin, B. Karimi, J. T. Peltonen, J. Ankerhold, and J. P. Pekola, Heat rectification via a superconducting artificial atom, *Communications Physics* **3**, 40 (2020).
- [2] I. Žutić, J. Fabian, and S. Das Sarma, Spintronics: Fundamentals and applications, *Rev. Mod. Phys.* **76**, 323 (2004).

- [3] S. Wolf, D. Awschalom, R. Buhrman, J. Daughton, v. S. von Molnár, M. Roukes, A. Y. Chtchelkanova, and D. Treger, Spintronics: a spin-based electronics vision for the future, *science* **294**, 1488 (2001).
- [4] K. Poulsen and N. T. Zinner, Giant magnetoresistance in boundary-driven spin chains, *Phys. Rev. Lett.* **126**, 077203 (2021).

- [5] K. Sääskilahti, J. Oksanen, and J. Tulkki, Thermal balance and quantum heat transport in nanostructures thermalized by local langevin heat baths, *Phys. Rev. E* **88**, 012128 (2013).
- [6] N. Li, J. Ren, L. Wang, G. Zhang, P. Hänggi, and B. Li, Colloquium: Phononics: Manipulating heat flow with electronic analogs and beyond, *Rev. Mod. Phys.* **84**, 1045 (2012).
- [7] N. A. Roberts and D. Walker, A review of thermal rectification observations and models in solid materials, *International Journal of Thermal Sciences* **50**, 648 (2011).
- [8] K. Ptaszyński and M. Esposito, Thermodynamics of quantum information flows, *Phys. Rev. Lett.* **122**, 150603 (2019).
- [9] Q. Bouton, J. Nettersheim, S. Burgardt, D. Adam, E. Lutz, and A. Widera, A quantum heat engine driven by atomic collisions, *Nature Communications* **12**, 2063 (2021).
- [10] A. Levy, R. Alicki, and R. Kosloff, Quantum refrigerators and the third law of thermodynamics, *Phys. Rev. E* **85**, 061126 (2012).
- [11] N. M. Myers, O. Abah, and S. Deffner, Quantum thermodynamic devices: From theoretical proposals to experimental reality, *AVS quantum science* **4**, <https://doi.org/10.1116/5.0083192> (2022).
- [12] D. Gelbwaser-Klimovsky, R. Alicki, and G. Kurizki, Minimal universal quantum heat machine, *Phys. Rev. E* **87**, 012140 (2013).
- [13] C. Wang, X.-M. Chen, K.-W. Sun, and J. Ren, Heat amplification and negative differential thermal conductance in a strongly coupled nonequilibrium spin-boson system, *Physical Review A* **97**, 052112 (2018).
- [14] J. Du, W. Shen, S. Su, and J. Chen, Quantum thermal management devices based on strong coupling qubits, *Physical Review E* **99**, 062123 (2019).
- [15] B.-q. Guo, T. Liu, and C.-s. Yu, Multifunctional quantum thermal device utilizing three qubits, *Physical Review E* **99**, 032112 (2019).
- [16] M. Majland, K. S. Christensen, and N. T. Zinner, Quantum thermal transistor in superconducting circuits, *Phys. Rev. B* **101**, 184510 (2020).
- [17] A. Mandarino, K. Joulain, M. D. Gómez, and B. Bellomo, Thermal transistor effect in quantum systems, *Phys. Rev. Appl.* **16**, 034026 (2021).
- [18] A. Mandarino, K. Joulain, M. D. Gómez, and B. Bellomo, Thermal transistor effect in quantum systems, *Physical Review Applied* **16**, 034026 (2021).
- [19] A. H. Malavazi, B. Ahmadi, P. Mazurek, and A. Mandarino, Detuning effects for heat-current control in quantum thermal devices, *Physical Review E* **109**, 064146 (2024).
- [20] Y.-j. Yang, Y.-q. Liu, Z. Liu, and C.-s. Yu, Magnetically controlled quantum thermal devices via three nearest-neighbor coupled spin-1/2 systems, *Phys. Rev. E* **109**, 014142 (2024).
- [21] D. Segal and A. Nitzan, Spin-boson thermal rectifier, *Phys. Rev. Lett.* **94**, 034301 (2005).
- [22] Y. Yan, C.-Q. Wu, and B. Li, Control of heat transport in quantum spin systems, *Phys. Rev. B* **79**, 014207 (2009).
- [23] T. Werlang, M. A. Marchiori, M. F. Cornelio, and D. Valente, Optimal rectification in the ultrastrong coupling regime, *Phys. Rev. E* **89**, 062109 (2014).
- [24] A. Marcos-Vicioso, C. López-Jurado, M. Ruiz-García, and R. Sánchez, Thermal rectification with interacting electronic channels: Exploiting degeneracy, quantum superpositions, and interference, *Phys. Rev. B* **98**, 035414 (2018).
- [25] D. Goury and R. Sánchez, Reversible thermal diode and energy harvester with a superconducting quantum interference single-electron transistor, *Applied Physics Letters* **115**, <https://doi.org/10.1063/1.5109100> (2019).
- [26] C. Kargı, M. T. Naseem, T. Opatrný, Ö. E. Müstecaplıođlu, and G. Kurizki, Quantum optical two-atom thermal diode, *Physical Review E* **99**, 042121 (2019).
- [27] V. Upadhyay, M. T. Naseem, R. Marathe, and Ö. E. Müstecaplıođlu, Heat rectification by two qubits coupled with dzyaloshinskii-moriya interaction, *Physical Review E* **104**, 054137 (2021).
- [28] F. Ivander, N. Anto-Sztrikacs, and D. Segal, Quantum coherence-control of thermal energy transport: the v model as a case study, *New Journal of Physics* **24**, 103010 (2022).
- [29] K. Poulsen, A. C. Santos, L. B. Kristensen, and N. T. Zinner, Entanglement-enhanced quantum rectification, *Phys. Rev. A* **105**, 052605 (2022).
- [30] S. Khandelwal, M. Perarnau-Llobet, S. Seah, N. Brunner, and G. Haack, Characterizing the performance of heat rectifiers, *Physical Review Research* **5**, 013129 (2023).
- [31] A. Rajapaksha, S. D. Gunapala, and M. Premaratne, Enhanced thermal rectification in coupled qutrit-qubit quantum thermal diode, *APL Quantum* **1**, 046123 (2024).
- [32] Y.-q. Liu, Y.-j. Yang, T.-t. Ma, Z. Liu, and C.-s. Yu, Quantum heat valve and diode of strongly coupled defects in amorphous material, *Phys. Rev. E* **109**, 014137 (2024).
- [33] A. Riera-Campenya, M. Mehboudi, M. Pons, and A. Sanpera, Dynamically induced heat rectification in quantum systems, *Physical Review E* **99**, 032126 (2019).
- [34] T. J. Alexander, High-heat-flux rectification due to a localized thermal diode, *Phys. Rev. E* **101**, 062122 (2020).
- [35] A. Iorio, E. Strambini, G. Haack, M. Campisi, and F. Gizotto, Photonic heat rectification in a system of coupled qubits, *Phys. Rev. Appl.* **15**, 054050 (2021).
- [36] M. A. Simón, A. Alaña, M. Pons, A. Ruiz-García, and J. G. Muga, Heat rectification with a minimal model of two harmonic oscillators, *Phys. Rev. E* **103**, 012134 (2021).
- [37] C. Stevenson and B. Braunecker, Decoupled heat and charge rectification as a many-body effect in quantum wires, *Phys. Rev. B* **103**, 115413 (2021).
- [38] S. Palafox, R. Román-Ancheyta, B. i. e. i. f. m. c. Çakmak, and O. E. Müstecaplıođlu, Heat transport and rectification via quantum statistical and coherence asymmetries, *Phys. Rev. E* **106**, 054114 (2022).
- [39] Y.-q. Liu, Y.-j. Yang, T.-t. Ma, and C.-s. Yu, Quantum heat valve and entanglement in superconducting lc resonators, *Applied Physics Letters* **123**, 144002 (2023).
- [40] A. Seif, W. DeGottardi, K. Esfarjani, and M. Hafezi, Thermal management and non-reciprocal control of phonon flow via optomechanics, *Nature Communications* **9**, [10.1038/s41467-018-03624-y](https://doi.org/10.1038/s41467-018-03624-y) (2018).
- [41] B. Bhandari, P. A. Erdman, R. Fazio, E. Paladino, and F. Taddei, Thermal rectification through a nonlinear quantum resonator, *Physical Review B* **103**, 155434 (2021).
- [42] L.-A. Wu and D. Segal, Sufficient conditions for thermal rectification in hybrid quantum structures, *Physical re-*

- view letters **102**, 095503 (2009).
- [43] N. Kalantar, B. K. Agarwalla, and D. Segal, Harmonic chains and the thermal diode effect, *Phys. Rev. E* **103**, 052130 (2021).
- [44] G. T. Landi, E. Novais, M. J. de Oliveira, and D. Karevski, Flux rectification in the quantum xxz chain, *Phys. Rev. E* **90**, 042142 (2014).
- [45] J. Ordonez-Miranda, Y. Ezzahri, and K. Joulain, Quantum thermal diode based on two interacting spinlike systems under different excitations, *Phys. Rev. E* **95**, 022128 (2017).
- [46] V. Balachandran, G. Benenti, E. Pereira, G. Casati, and D. Poletti, Heat current rectification in segmented xxz chains, *Phys. Rev. E* **99**, 032136 (2019).
- [47] J. J. Mendoza-Arenas and S. R. Clark, Giant rectification in strongly interacting driven tilted systems, *PRX Quantum* **5**, 010341 (2024).
- [48] V. Balachandran, G. Benenti, E. Pereira, G. Casati, and D. Poletti, Perfect diode in quantum spin chains, *Phys. Rev. Lett.* **120**, 200603 (2018).
- [49] J.-H. Jiang, M. Kulkarni, D. Segal, and Y. Imry, Phonon thermoelectric transistors and rectifiers, *Phys. Rev. B* **92**, 045309 (2015).
- [50] A. A. Aligia, D. P. Daroca, L. Arrachea, and P. Roura-Bas, Heat current across a capacitively coupled double quantum dot, *Phys. Rev. B* **101**, 075417 (2020).
- [51] M. Xu, J. T. Stockburger, and J. Ankerhold, Heat transport through a superconducting artificial atom, *Phys. Rev. B* **103**, 104304 (2021).
- [52] H. Huebl, C. W. Zollitsch, J. Lotze, F. Hocke, M. Greifenstein, A. Marx, R. Gross, and S. T. B. Goennenwein, High cooperativity in coupled microwave resonator ferromagnetic insulator hybrids, *Phys. Rev. Lett.* **111**, 127003 (2013).
- [53] Y. Tabuchi, S. Ishino, T. Ishikawa, R. Yamazaki, K. Usami, and Y. Nakamura, Hybridizing ferromagnetic magnons and microwave photons in the quantum limit, *Phys. Rev. Lett.* **113**, 083603 (2014).
- [54] D. Lachance-Quirion, Y. Tabuchi, A. Glorpe, K. Usami, and Y. Nakamura, Hybrid quantum systems based on magnonics, *Applied Physics Express* **12**, 070101 (2019).
- [55] J. Li, Y.-P. Wang, W.-J. Wu, S.-Y. Zhu, and J. You, Quantum network with magnonic and mechanical nodes, *PRX Quantum* **2**, 040344 (2021).
- [56] C. A. Potts, E. Varga, V. A. S. V. Bittencourt, S. V. Kusminskiy, and J. P. Davis, Dynamical backaction magnomechanics, *Phys. Rev. X* **11**, 031053 (2021).
- [57] X. Zhang, C.-L. Zou, L. Jiang, and H. X. Tang, Strongly coupled magnons and cavity microwave photons, *Phys. Rev. Lett.* **113**, 156401 (2014).
- [58] A. Osada, R. Hisatomi, A. Noguchi, Y. Tabuchi, R. Yamazaki, K. Usami, M. Sadgrove, R. Yalla, M. Nomura, and Y. Nakamura, Cavity optomagnonics with spin-orbit coupled photons, *Phys. Rev. Lett.* **116**, 223601 (2016).
- [59] Y. Tabuchi, S. Ishino, A. Noguchi, T. Ishikawa, R. Yamazaki, K. Usami, and Y. Nakamura, Quantum magnonics: The magnon meets the superconducting qubit, *Comptes Rendus Physique* **17**, 729 (2016).
- [60] H. Yuan, Y. Cao, A. Kamra, R. A. Duine, and P. Yan, Quantum magnonics: When magnon spintronics meets quantum information science, *Physics Reports* **965**, 1 (2022), quantum magnonics: When magnon spintronics meets quantum information science.
- [61] M. S. Ebrahimi, A. Motazedifard, and M. B. Harouni, Single-quadrature quantum magnetometry in cavity electromagnonics, *Phys. Rev. A* **103**, 062605 (2021).
- [62] C. O. Edet, M. Asjad, D. Dutykh, N. Ali, and O. Abah, Entropy production rate and correlations in a cavity magnomechanical system, *Phys. Rev. Res.* **6**, 033037 (2024).
- [63] N. Crescini, C. Braggio, G. Carugno, R. Di Vora, A. Ortolan, and G. Ruoso, Magnon-driven dynamics of a hybrid system excited with ultrafast optical pulses, *Communications Physics* **3**, 164 (2020).
- [64] F.-X. Sun, S.-S. Zheng, Y. Xiao, Q. Gong, Q. He, and K. Xia, Remote generation of magnon schrödinger cat state via magnon-photon entanglement, *Phys. Rev. Lett.* **127**, 087203 (2021).
- [65] V. Gorini, A. Kossakowski, and E. C. G. Sudarshan, Completely positive dynamical semigroups of n -level systems, *Journal of Mathematical Physics* **17**, 821 (1976).
- [66] G. Lindblad, On the generators of quantum dynamical semigroups, *Communications in Mathematical Physics* **48**, 119 (1976).
- [67] H.-P. Breuer and F. Petruccione, *The theory of open quantum systems* (Oxford University Press, USA, 2002).
- [68] G. T. Landi, Quantum information and quantum noise, en. graduate course in Quantum Information and Quantum noise (2018).
- [69] G. De Chiara, G. Landi, A. Hewgill, B. Reid, A. Ferraro, A. J. Roncaglia, and M. Antezza, Reconciliation of quantum local master equations with thermodynamics, *New Journal of Physics* **20**, 113024 (2018).
- [70] K. Joulain, J. Drevillon, Y. Ezzahri, and J. Ordonez-Miranda, Quantum thermal transistor, *Physical review letters* **116**, 200601 (2016).
- [71] T. Ruokola, T. Ojanen, and A.-P. Jauho, Thermal rectification in nonlinear quantum circuits, *Physical Review B—Condensed Matter and Materials Physics* **79**, 144306 (2009).
- [72] J. Li, S.-Y. Zhu, and G. Agarwal, Magnon-photon-phonon entanglement in cavity magnomechanics, *Physical review letters* **121**, 203601 (2018).